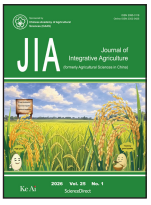
Journal of Integrative Agriculture 2026, 25(1): 235–246

Available online at ScienceDirect

Journal of Integrative Agriculture



RESEARCH ARTICLE

Novel characterization of NADC30-like and NADC34-like PRRSV strains in China: Epidemiological status and pathogenicity analysis of L1A variants

Hu Xu[1*], Siyu Zhang[1*], Zhenyang Guo[1*], Chao Li[1], Bangjun Gong[1], Jinhao Li[1], Qi Sun[1], Jing Zhao[1], Menglin Zhang[1], Lirun Xiang[1], Yandong Tang[1], Chaoliang Leng[2], Jianan Wu[1], Qian Wang[1], Jinmei Peng[1], Guohui Zhou[1], Huairan Liu[1], Tongqing An[1], Xuehui Cai[1], Zhijun Tian[1#], Hongliang Zhang[1#]

[1] *State Key Laboratory of Veterinary Biotechnology, Harbin Veterinary Research Institute, Chinese Academy of Agricultural Sciences, Harbin 150001, China*

[2] *Henan Provincial Engineering and Technology Center of Animal Disease Diagnosis and Integrated Control, Nanyang Normal University, Nanyang 473061, China*

Highlights

- A novel PRRSV L1A variant, characterized by a unique recombination pattern derived from NADC30-like, NADC34-like, and HP-like strains, has emerged as a circulating strain in China.
- Epidemiological analyses indicate that L1A variants have spread rapidly and are now prevalent in at least 12 provinces across China.
- The L1A variant exhibits moderate pathogenicity in piglets, characterized by persistent fever, impaired weight gain, severe pulmonary lesions, and prolonged viremia with high viral loads.

Abstract

NADC34-like porcine reproductive and respiratory syndrome virus (PRRSV), which first appeared in China in 2017, is currently one of the main epidemic strains in China. In this study, we found that a new variant of NADC34-like PRRSV evolved, named the L1A variant. The phylogenetics, epidemic status, and pathogenicity of the LA variants were subsequently comprehensively evaluated. Based on the results of the ORF5 phylogenetic analysis, the L1A variants were classified as NADC34-like PPRSV. All the strains had the same discontinuous 131-aa deletion in the NSP2 region (similar to that in the NADC30). Recombination analysis revealed that the L1A variants were recombinant viruses that contained an NADC30-like PRRSV skeleton, a nonstructural protein-encoding gene region obtained in part from JXA1-like PRRSV and a ORF2-ORF6 gene region partly obtained from NADC34-like PRRSV and that exhibited similar recombination patterns. We successfully isolated the L1A variant TZJ2756 from PAMs and Marc-145 cells. In animal experiments, TZJ2756 exhibited moderate pathogenicity in piglets, causing obvious clinical symptoms, namely, persistent fever, significantly reduced body weight, interstitial edema and severe interstitial pneumonia in the lungs, and prolonged high-load viremia. L1A variants have been detected in at least 12 provinces in China and share many similar epidemiological characteristics with the American L1C variant. This research will enhance our understanding of the prevalence of L1A variants and furnish valuable data for the ongoing monitoring of NADC34-like PRRSV in China.

Keywords: NADC34-like porcine reproductive and respiratory syndrome virus (PRRSV), NADC30-like PRRSV, L1A variant, recombination, pathogenicity

Received 1 December 2023; Received in revised form 4 February 2024; Accepted 15 Feburary 2024; Available online 16 March 2024
Hu Xu, E-mail: xuhu1995@foxmail.com; Siyu Zhang, E-mail: zhangsiyucaas@163.com; [#]Correspondence Zhijun Tian, E-mail: tianzhijun@caas.com; Hongliang Zhang, E-mail: zhanghongliang01@caas.cn

[*] These authors contributed equally to this work.

© 2026 CAAS. Publishing services by Elsevier B.V. on behalf of KeAi Communications Co. Ltd. This is an open access article under the CC BY-NC-ND license (http://creativecommons.org/licenses/by-nc-nd/4.0/). Peer review under responsibility of Editorial Board of *Journal of Integrative Agriculture*.
doi: 10.1016/j.jia.2024.03.056

1. Introduction

Porcine reproductive and respiratory syndrome (PRRS) is a highly significant and destructive infectious disease in the commercial pig farming industry that has significant economic consequences (Nathues *et al.* 2017). PRRS virus (PRRSV), which is responsible for causing PRRS, is an enveloped, positive-sense RNA virus categorized under the order *Nidovirales* and the family *Arteriviridae* (Brinton *et al.* 2021). The genome size was estimated to be approximately 15 kb, consisting of a 5′-untranslated region (UTR), at least 11 overlapping open reading frames (ORFs), and a 3′-poly(A) tail (Li *et al.* 2015). PRRSV can be divided into two species: *Betaarterivirus suid* 1 (PRRSV-1) and *Betaarterivirus suid* 2 (PRRSV-2) (Sun *et al.* 2023). Since the initial identification of PRRSV in China in 1996, the PRRSV-2 strain has consistently prevailed as the primary circulating strain within the country (Guo *et al.* 2018).

The extensive genetic diversity exhibited by PRRSV is a notable trait. In 2010, Shi *et al.* (2010a, b) developed a global classification system for PRRSV by conducting a comprehensive analysis of the ORF5 gene sequence. According to this system, PRRSV-2 is classified into nine lineages (Lineages 1-9), each containing several sublineages. At present, PRRSV Lineage 1 is the most widely distributed and genetically complex lineage in the world (Paploski *et al.* 2021; Zhang *et al.* 2022; Kim *et al.* 2023; Lee *et al.* 2023; Yim-im *et al.* 2023). In 2021, American researchers used more than 20,000 ORF5 gene sequences to further divide PRRSV Lineage 1 into 8 sublineages, L1A-L1H (Paploski *et al.* 2021). In China, two sublineages of PRRSV-2 Lineage 1 strains, namely, NADC30-like (L1.8/L1C) and NADC34-like (L1.5/L1A), have been identified, and these strains were initially discovered in China in 2012 and 2017, respectively (Zhou *et al.* 2015; Zhang *et al.* 2018). NADC30-like PRRSV strains with a discontinuous 131-aa (322–432, 483 and 504–522) deletion in Nsp2 have gradually become the dominant strains in recent years (Guo *et al.* 2019). NADC34-like PRRSV carried a genetic marker of a 100-aa deletion at positions 328–427 of the Nsp2 gene of VR2332 (Xu *et al.* 2020). In recent years, NADC34-like PRRSV strains have rapidly spread throughout China and are currently the predominant circulating strains of PRRSV-2, along with the NADC30-like and HP-PRRSV strains (Xu *et al.* 2022a; Zhao *et al.* 2022).

Recombination events in PRRSV are common and occur frequently within and/or between lineages, resulting in the emergence of new PRRSV variants and changes in the viral pathogenicity (Cui *et al.* 2022). However, widespread PRRSV strains with the same recombination pattern have rarely been reported. In the autumn of 2020, pig producers in the midwestern U.S. experienced atypical production losses caused by the RFLP 1-4-4 L1C variant strain (MW887655) (Kikuti *et al.* 2021; Trevisan *et al.* 2021a). The RFLP 1-4-4 L1C variant strains are derived from the recombination of L1C (NADC30-like) and L1A (NADC34-like) PRRSV strains, which have a great impact on the local pig industry, and these strains share high homology and the same recombination pattern (Pamornchainavakul *et al.* 2022). With the rapid spread of NADC34-like PRRSV strains in China, the number of reports on these strains has increased. The characteristics of the NADC34-like PRRSV strains currently circulating in China and whether they share similar genomic features with the U.S. L1C variant strain remain unclear.

In this study, we discovered that NADC34-like PRRSV has undergone 7 years of evolution in China, resulting in the emergence of a new variant strain, which was named the L1A variant. We further sequenced the whole genomes of eight L1A variants, comprehensively analyzed their whole-genome characteristics, and evaluated their pathogenicity.

2. Materials and methods

2.1. Sample collection and genome sequencing

Our laboratory has monitored the prevalence of PRRSV in China for a long time. Since the discovery of NADC34-like PRRSV recombined with local NADC30-like strains in China in 2020, increasing numbers of NADC34-like PRRSVs with the same discontinuous 131-aa deletion in the Nsp2 region as in the NADC30 strain have been reported. To explore the genome-wide characteristics and pathogenicity of the newly isolated NADC34-like PRRSV strains with a discontinuous a 131-aa discontinuous deletion in the Nsp2 region from 2021 to October 2023, clinical samples positive for new NADC34-like PRRSV were collected from 8 pig farms in 4 regions, namely, Inner Mongolia, Liaoning, Heilongjiang and Henan (Table 1). Tissue sample processing, RNA extraction, cDNA preparation, and RT-PCR were conducted following previously described methods (Zhang *et al.* 2019). The primers used to detect the PRRSV ORF5 gene and amplify entire gene sequences were described previously (Zhang *et al.* 2019). Following PCR, the products were purified using a gel extraction kit from Omega (USA) and subsequently cloned and inserted into the PMD18-T cloning vector from TaKaRa (Japan). Transformation of the cloned products was carried out using DH5α competent cells from Shenggong (China), and three positive clones for each fragment were chosen for Sanger sequencing at Ruibiotech (China). The obtained sequences were subsequently assembled using Lasergene software provided by DNASTAR, Inc.

2.2. Sequence analysis and phylogenetic analysis

The ClustalW algorithm, implemented in MegAlign in Lasergene Software (DNASTAR, Inc.), was used for amino acid sequence alignment. The ORF5 and whole-genome sequences of reference strains sourced from the GenBank database and PRRSV strains obtained during this study were aligned using MEGA7 and MAFFT, respectively (Katoh and Standley 2013; Kumar *et al.* 2016). MEGA7.0 software was used for molecular evolutionary analyses and construction of phylogenetic trees *via* the neighbor-joining method with 1,000 bootstrap replications (Kumar *et al.* 2016). The resulting phylogenetic tree was annotated using FigTree (v1.4.4) software.

To assess recombination, the alignment was subjected to screening using RDP4 software (Murtaugh *et al.* 2010). Seven different algorithms (RDP, GeneConv, BootScan, MaxChi, Chimera, SiScan, and 3Seq) with Bonferroni correction were

Table 1 Information of all reported whole genome L1A variant strains

Taxa	Accession no.	Regions	Clinical signs	Isolation date	RFLP pattern	References
TZJ2165	OL516356	Heilongjiang	Unknown	2021	1-4-2	This study
WK621	OQ790147	Inner Mongolia	Sow abortion rate of 20% and piglet mortality rate of 20%	2022	1-4-2	This study
TZJ2451	OQ790146	Liaoning	Unknown	2022	1-4-2	This study
TZJ2756	OQ748875	Liaoning	Sow abortion rate of 40% and piglet mortality rate of 50%	2023	1-7-2	This study
WK730	OR826314	Heilongjiang	Sow abortion rate of 40% and piglet mortality rate of 20%	2023	1-7-1	This study
TZJ3005	OR826313	Liaoning	Sow abortion rate of 20%	2023	1-5-4	This study
TZJ3115	OR826315	Henan	Unknown	2023	1-3-4	This study
TZJ3116	OR826316	Henan	Sow abortion rate of 20%	2023	1-7-4	This study
BJ20-06	MZ047780	Beijing	Unknown	2020	1-4-4	Not found
JS2020	MZ342900	Jiangsu	Unknown	2020	1-7-4	Not found
PRRSV-China/SCcd2020/2020	MW803134	Sichuan	Morbidity was about 75%, with a mortality of 15%	2020	1-7-4	Zhou *et al.* (2023)
SDlz20-04	MZ047781	Shandong	Unknown	2020	1-4-4	Not found
YC-2020	ON180781	Shanxi	Unknown	2020	1-7-4	Zhao *et al.* (2023)
GXQZ20210403	OK486523	Guangxi	Unknown	2021	1-7-4	Wang *et al.* (2022)
PRRSV/CN/FJGD01/2021	OL310959	Fujian	Sow abortion rate of 20% and piglet mortality rate of 10%	2021	1-6-4	Liu *et al.* 2022)
GD-H1	ON691479	Guangdong	Unknown	2021	1-7-4	Wu *et al.* (2022)
GD-F1	ON691480	Guangdong	Unknown	2021	1-5-4	Wu *et al.* (2022)
CH-HNPY-01/2022	OP716076	Henan	Unknown	2022	1-5-4	Not found

employed to test for potential recombination events. Detection by four or more of these methods implemented in RDP4 was considered significant evidence of recombination (Shi *et al.* 2013). To summarize the recombination patterns of the strains, representative L1A (IA/2014/NADC34, accession: MF326985.1), L1C (NADC30, accession: JN654459.1), L8.7 (JXA1, accession: EF112445.1), L3.5 (QYYZ, accession: JQ308798.1), and L5.1 (VR2332, accession: EF536003.1) strains were selected as reference strains for recombination analysis. The virus strains that did not participate in the recombination were then deleted to determine the final recombination location. Recombination events were further identified using Simplot v 3.5.1, and boot scanning analysis was conducted with a 200-bp window, sliding along the genome alignment with a step size of 20 bp.

The genetic diversity of new PRRSV strains has been characterized using restriction fragment length polymorphism (RFLP) typing, which is based on the cleavage patterns of ORF5 obtained with three restriction enzymes (*Mlu*I, *Hinc*II, and *Sac*II) (Trevisan *et al.* 2021b).

2.3. Virus isolation

Primary alveolar macrophages (PAMs) were derived from 5-wk-old specific-pathogen-free (SPF) pigs and maintained in RPMI 1640 medium (Gibco BRL Co., Ltd., USA) supplemented with 10% fetal bovine serum (FBS; OPCEL., China) (de Abin *et al.* 2009). The PRRSV-positive sample suspensions were filtered through 0.22-μm filters and subsequently inoculated onto PAMs and Marc-145 cells (an African green monkey kidney cell line) to isolate the virus (Zhang *et al.* 2019). After three days, the cultures were harvested and stored as viral stocks at –80°C. Cultures from PAMs after the third passage were utilized for animal experiments. The viral titer was determined using methods described previously (Song *et al.* 2020).

2.4. Immunofluorescence assays

Immunofluorescence assays (IFAs) were performed following a previously described protocol (Leng *et al.* 2012). PAMs and Marc-145 cells were inoculated with the PRRSV isolate TZJ2756 (GenBank accession: OQ748875.1) to prepare viral antigens. Monoclonal antibodies against PRRSV-2 1H4 were added to the cells, which were subsequently incubated for 30 min (Li *et al.* 2022). After three washes with PBS, the cells were incubated with FITC-conjugated goat anti-mouse IgG antibody (Sigma, USA) and secondary antibodies for 30 min. The cells were then washed three times with PBS and examined under a fluorescence microscope in PBS.

2.5. Animal experiments

Eight 6-wk-old SPF piglets were randomly assigned to two groups, a challenge group (n=5) and a control group (n=3), and were housed individually in biosafety rooms. The piglets in the challenge group and those in the control group were intramuscularly (2 mL) and intranasally (2 mL) administered TZJ2756 (1×10^5 $TCID_{50}$ mL^{-1}, 4 mL per pig) and RPMI 1640, respectively. Throughout the duration of the experiment, the rectal body temperatures and clinical signs of the piglets were documented on a daily basis. Additionally, the body weight of each piglet was measured weekly.

Blood samples were collected at 0, 3, 7, 10, 14, 17, and 21 days post inoculation (dpi) for viremia detection using a real-time quantitative PCR (RT-qPCR) method developed by our laboratory (Song *et al.* 2020). All the pigs were euthanized at d 21 dpi, and tissue samples were obtained from the heart, liver, spleen, lungs, kidneys, submaxillary

lymph nodes, tonsils, small intestine, bladder, and stomach for virus detection *via* RT-qPCR. Furthermore, at 21 dpi, lung and submaxillary lymph node samples were obtained from each piglet. These samples were fixed in a 4% formaldehyde solution and subsequently prepared for histopathological analysis *via* hematoxylin and eosin staining.

2.6. Serological testing

PRRSV-specific antibodies were assessed using a commercially available ELISA Kit (IDEXX, Inc., Westbrook, ME, USA) according to the manufacturer's instructions. According to the manufacturer's guidelines, sample-to-positive control (S/P) ratios exceeding 0.4 were considered indicative of a positive result.

2.7. Statistical analysis

To determine significant differences between the two groups, a *t*-test (and nonparametric tests) was conducted using GraphPad 6.0 (San Diego, CA, USA). The significance level was set to $P<0.05$.

3. Results

3.1. Sample collection and whole-genome sequencing

In this study, new NADC34-like PRRSV-positive samples were collected from 8 pig farms in 4 regions in China from 2021 to 2023 (Table 1). The genomes of these isolates were 15,001–15,020 nt in length, excluding 3′ poly (A) tails. The clinical incidence of some positive samples is shown in Table 1, among which the TZJ2756 strain exhibited the most severe clinical manifestations.

3.2. Phylogenetic analysis and distribution of L1A variants

To establish genetic relationships between newly expressed NADC34-like PRRSV and other PRRSV isolates, phylogenetic trees were constructed based on the ORF5 gene sequences. Analysis of the ORF5 gene sequences revealed that all the newly isolated NADC34-like PRRSV strains formed a separate clade similar to that of the US L1C variant, and the strains in this clade were named L1A variants (Fig. 1-A). To analyze the genetic characteristics of the L1A variant in more detail, we obtained all the complete genome sequences of L1A and L1C PRRSV from GenBank. By conducting a phylogenetic analysis, we found that the L1A variants were classified as L1C (NADC30-like) and formed a separate clade, which indicates that the L1A variant is a new type of recombinant virus (Fig. 1-B). As of November 2023, a total of 18 PRRSV strains with available whole-genome sequences, including strains TZJ2165, TZJ2451, TZJ2756, TZJ3005, TZJ3115, TZJ3116, WK621 and WK730, were classified as L1A variants (Table 1).

Taken together, the information from this study and from GenBank indicated that L1A variant strains have been found in at least 12 regions in China, including Heilongjiang, Inner Mongolia, Liaoning, Beijing, Henan, Guangxi, Jiangsu, Sichuan, Fujian, Shandong and Shanxi, as of October 2023. These regions cover most of the major pig-producing provinces in China (Table 1).

3.3. Recombination analysis

The recombination events in the new L1A variants were analyzed using SimPlot and RDP4, and the results indicated that the new L1A variants (TZJ2165, TZJ2451, TZJ2756, TZJ3005, TZJ3115, TZJ3116, WK621 and WK730) were all recombinant viruses that originated from a combination of NADC30-like PRRSV (L1C), NADC34-like PRRSV (L1A) and JXA1-like PRRSV (L8.7). The specific recombination locations and fragment sizes are shown in Table 2. According to a similarity plot, these new L1A variants exhibit very similar recombination characteristics (Appendix A). All of these strains have two similar recombination fragments (A and B). New L1A variants were primarily derived from NADC30-like PRRSV with recombination of JXA1-like PRRSV in certain nonstructural protein regions (fragment A) and recombination of the NADC34-like strain in certain structural protein regions (fragment B) (Appendix A); fragment A is located in the Nsp3-NSP9 region, whereas fragment B is located in the ORF2-ORF6 region. The TZJ2165, TZJ2451, TZJ2756, TZJ3115 and TZJ3116 strains also exhibited additional recombination with JXA1-like PRRSV in the Nsp1 and Nsp2 regions (Appendix A).

To determine the recombination patterns of the L1A variant strains, we further analyzed the recombination modes of all the L1A variant strains with complete genome sequences available in the GenBank database (Table 2). These strains also had two recombination fragments (A and B), similar to the L1A variant found in this study (Table 2). Therefore, the L1A variant strain is a novel recombinant PRRSV with similar recombination characteristics in the Nsp3-Nsp9 region and ORF2-ORF6 (Fig. 1-C).

3.4. NSP2 amino acid and RFLP analysis

Amino acid sequence alignment revealed that, compared with that of VR2332, the L1A variant exhibited a discontinuous deletion of 131 (111+1+19) amino acids in Nsp2, similar to what was observed in the NADC30 strain, specifically at positions 322–432 aa, 483 aa, and 504–522 aa (Fig. 1-E). In contrast, the L1C variant harbors a continuous 100-aa deletion at residues 328–427 of VR-2332 Nsp2, which is consistent with the patterns observed for IA/2014/NADC34 (Fig. 1-E). This finding is consistent with the results of the recombination analysis.

The results of the RFLP pattern analysis showed that the L1A variants did not exhibit consistent RFLP patterns; the patterns included 1-4-2, 1-3-4, 1-4-4, and 1-7-4 (Table 1). Therefore, the L1A variant had the same Nsp2 amino-acid-deletion characteristics but did not form a unified RFLP pattern.

3.5. Virus isolation and homology comparison

To assess the pathogenicity of the Chinese L1A variant strains, tissue homogenates from samples containing L1A variants were introduced into PAMs and Marc-145 cells in this study. However, the IFA results revealed that only the TZJ2756 strain was able to replicate in PAMs and Marc-145 cells for three consecutive passages (Fig. 2).

Full-length genome sequence alignment revealed that the L1A variant shared 85.0–86.4% sequence identity with IA/2014/NADC34, 88.7–90.7% identity with NADC30, and 83.4–85.9%

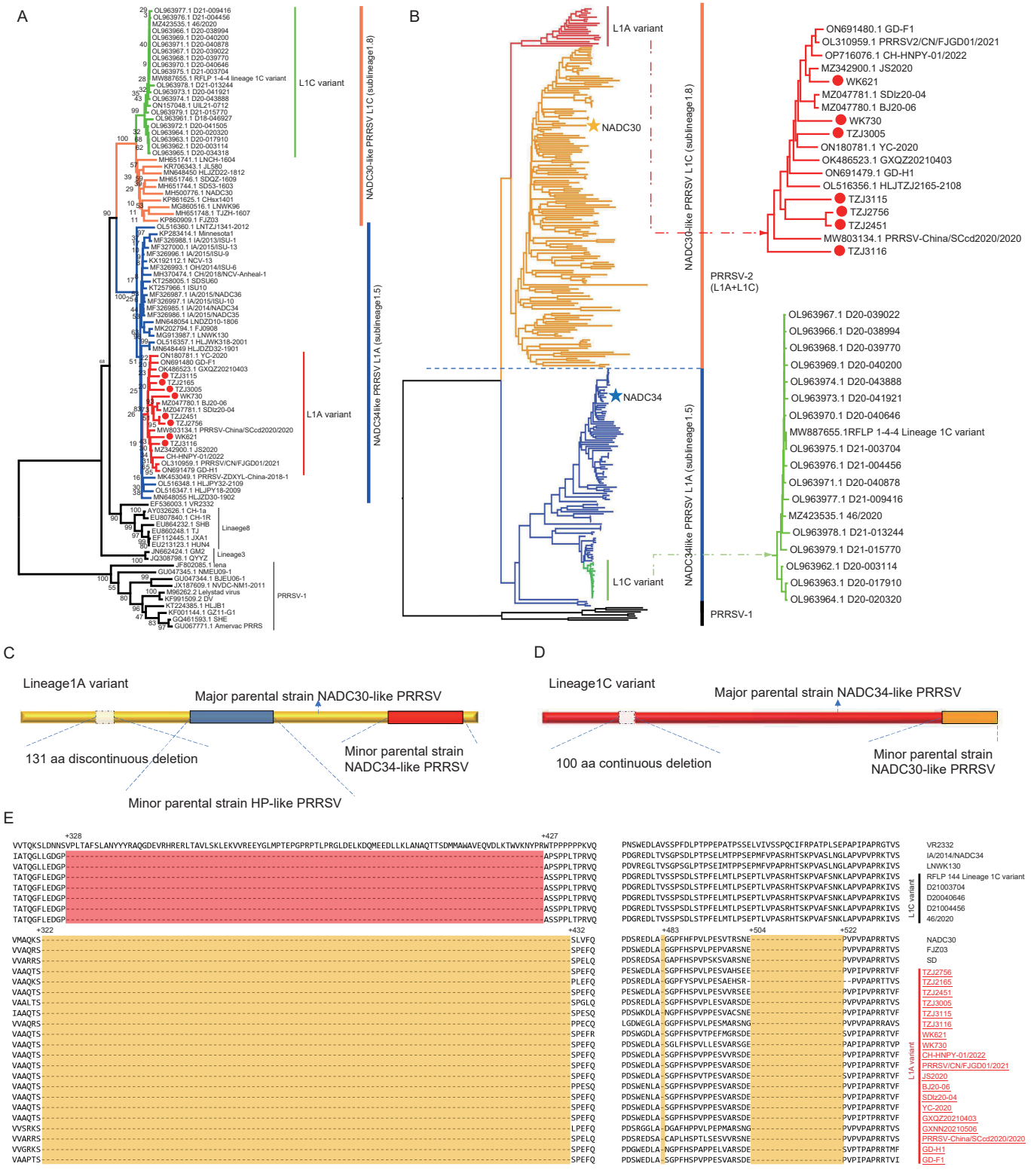


Fig. 1 Phylogenetic analysis, deduced amino acid sequence alignment of Nsp2 and virus recombination diagram of the L1A variant. A, phylogenetic tree constructed based on the ORF5 gene of novel L1A variant isolates and reference respiratory syndrome virus (PRRSV) strains from each lineage. B, phylogenetic tree constructed based on the full-length genomes of Chinese PRRSV L1A variant isolates and all whole-genome sequences of the PRRSV L1A and L1C strains worldwide. The red branches represent Chinese L1A variant strains, the blue branches represent L1A (NADC34-like) strains, and the orange branch represents L1C (NADC30-like) strains. The new whole-genome sequence obtained in this study is represented by red circles (●). Schematic diagram of the recombination of the Chinese L1A variant (C) and American L1C variant (D) strains. The blue color represents JXA1-like PRRSV, the yellow color represents NADC30-like PRRSV, and the red color represents NADC34-like PRRSV. The white area indicates the absence of characteristic amino acids. E, identification of PRRSV strains with an amino-acid deletion in Nsp2. The red color indicates the continuous deletion of 100 amino acids. The yellow color shows the discontinuous deletion of 131 amino acids.

Table 2 Information on recombination events of L1A variant detected by RPD4 software[1)]

Strains	Breakpoints		Parental sequence		Detection methods (*P*-value)						
	Beginning	Ending	Minor	Major	RDP	Geneconv	BootScan	MaxChi	Chimaera	SiScan	3Seq
WK730	5,095	7,681	JXA1	NADC30	6.510×10^{-48}	2.609×10^{-31}	2.113×10^{-46}	4.709×10^{-17}	2.859×10^{-20}	4.994×10^{-18}	1.332×10^{-15}
	11,675	14,056	IA/2014/ NADC34	NADC30	1.246×10^{-49}	1.516×10^{-21}	6.227×10^{-51}	1.958×10^{-21}	4.261×10^{-16}	–	3.330×10^{-16}
TZJ3005	4,923	7,658	JXA1	NADC30	2.472×10^{-43}	–	2.819×10^{-43}	1.247×10^{-17}	8.188×10^{-21}	3.536×10^{-18}	1.776×10^{-15}
	11,737	14,039	IA/2014/ NADC34	NADC30	8.221×10^{-52}	1.502×10^{-30}	1.546×10^{-52}	9.697×10^{-23}	4.441×10^{-24}	–	3.330×10^{-16}
TZJ2756	271	1,968	JXA1	NADC30	6.324×10^{-72}	1.727×10^{-57}	1.252×10^{-73}	7.692×10^{-30}	3.198×10^{-36}	–	4.409×10^{-08}
	5,066	7,694	JXA1	NADC30	1.490×10^{-37}	1.089×10^{-21}	5.963×10^{-36}	2.859×10^{-15}	4.773×10^{-06}	–	3.330×10^{-16}
	11,672	14,215	IA/2014/ NADC34	NADC30	3.994×10^{-53}	8.196×10^{-33}	5.183×10^{-55}	6.495×10^{-22}	1.918×10^{-18}	–	3.330×10^{-16}
WK621	4,923	7,678	JXA1	NADC30	1.294×10^{-45}	3.698×10^{-27}	6.919×10^{-45}	3.209×10^{-18}	1.230×10^{-12}	2.274×10^{-18}	1.776×10^{-15}
	11,982	14,059	IA/2014/ NADC34	NADC30	1.229×10^{-46}	2.824×10^{-23}	1.684×10^{-48}	4.456×10^{-21}	2.427×10^{-17}	–	3.330×10^{-16}
TZJ2451	141	2,097	JXA1	NADC30	9.628×10^{-78}	1.235×10^{-67}	2.034×10^{-77}	5.580×10^{-34}	1.778×10^{-36}	1.316×10^{-34}	1.332×10^{-15}
	4,905	7,664	JXA1	NADC30	1.486×10^{-62}	2.961×10^{-23}	2.410×10^{-64}	2.595×10^{-24}	2.790×10^{-16}	2.940×10^{-37}	6.217×10^{-15}
	11,743	14,285	IA/2014/ NADC34	NADC30	3.890×10^{-22}	3.975×10^{-13}	4.314×10^{-22}	2.662×10^{-05}	1.759×10^{-02}	9.375×10^{-35}	-
TZJ2165	1	698	JXA1	NADC30	–	3.712×10^{-17}	4.374×10^{-33}	3.046×10^{-12}	7.655×10^{-14}	1.552×10^{-09}	1.776×10^{-19}
	4,876	7,666	JXA1	NADC30	5.284×10^{-87}	3.083×10^{-41}	1.008×10^{-87}	4.893×10^{-34}	5.703×10^{-12}	5.731×10^{-35}	1.776×10^{-15}
	11,708	14,019	IA/2014/ NADC34	NADC30	4.268×10^{-61}	4.525×10^{-47}	6.682×10^{-59}	2.631×10^{-23}	2.498×10^{-24}	–	1.110×10^{-16}
TZJ3115	660	2,020	JXA1	NADC30	8.137×10^{-100}	8.278×10^{-101}	1.410×10^{-96}	5.805×10^{-37}	1.564×10^{-02}	–	–
	4,884	7,668	JXA1	NADC30	2.969×10^{-46}	1.009×10^{-14}	4.231×10^{-46}	2.840×10^{-20}	7.347×10^{-22}	–	4.440×10^{-16}
	12,305	14,051	IA/2014/ NADC34	NADC30	4.402×10^{-27}	1.511×10^{-13}	4.457×10^{-26}	5.511×10^{-10}	9.347×10^{-08}	9.702×10^{-13}	1.332×10^{-15}
TZJ3116	1,463	2,001	JXA1	NADC30	3.683×10^{-36}	8.223×10^{-10}	7.259×10^{-36}	1.404×10^{-12}	3.974×10^{-19}	–	1.091×10^{-11}
	4,910	7,679	JXA1	NADC30	6.384×10^{-70}	6.699×10^{-27}	1.344×10^{-69}	2.027×10^{-31}	6.862×10^{-36}	–	4.440×10^{-16}
	11,670	14051	IA/2014/ NADC34	NADC30	4.449×10^{-54}	2.147×10^{-27}	3.822×10^{-54}	6.344×10^{-22}	2.107×10^{-17}	–	3.330×10^{-16}
BJ20-06	4,920	7677	JXA1	NADC30	1.019×10^{-96}	1.435×10^{-41}	2.834×10^{-97}	6.615×10^{-32}	6.921×10^{-37}	2.047×10^{-33}	1.776×10^{-15}
	11,685	14217	IA/2014/ NADC34	NADC30	1.647×10^{-61}	5.405×10^{-42}	1.208×10^{-61}	1.008×10^{-05}	1.122×10^{-18}	–	4.440×10^{-16}
CH-HNPY-01/2022	4,919	7665	JXA1	NADC30	4.058×10^{-47}	2.688×10^{-30}	5.478×10^{-47}	2.351×10^{-20}	6.862×10^{-23}	–	1.110×10^{-16}
	11,671	14052	IA/2014/ NADC34	NADC30	1.315×10^{-52}	1.601×10^{-32}	6.001×10^{-54}	1.835×10^{-21}	1.409×10^{-03}	–	3.330×10^{-16}
GD-F1	4,887	7,677	JXA1	NADC30	2.017×10^{-82}	1.621×10^{-27}	6.399×10^{-84}	8.022×10^{-34}	9.936×10^{-14}	2.268×10^{-34}	1.776×10^{-15}
	11,736	14,055	IA/2014/ NADC34	NADC30	8.579×10^{-56}	4.045×10^{-36}	1.465×10^{-57}	9.352×10^{-21}	3.954×10^{-22}	–	4.440×10^{-16}
GD-H1	4,922	7,668	JXA1	NADC30	3.969×10^{-47}	1.050×10^{-24}	6.572×10^{-44}	3.320×10^{-20}	5.208×10^{-13}	–	1.110×10^{-16}
	11,674	14,114	IA/2014/ NADC34	NADC30	1.662×10^{-47}	7.422×10^{-27}	1.233×10^{-49}	9.058×10^{-04}	2.353×10^{-04}	–	3.330×10^{-16}
GXQZ20210403	651	1,331	JXA1	NADC30	1.032×10^{-49}	1.718×10^{-38}	1.228×10^{-50}	2.957×10^{-21}	3.374×10^{-22}	–	–

(Continued on next page)

Table 2 (Continued from preceding page)

Strains	Breakpoints		Parental sequence		Detection methods (*P*-value)					
	Beginning	Ending	Minor	Major	RDP	Geneconv	BootScan	MaxChi	Chimaera	SiScan	3Seq
	4,905	7,667	JXA1	NADC30	2.219×10^{-43}	2.826×10^{-36}	1.813×10^{-44}	6.044×10^{-32}	2.704×10^{-08}	–	4.440×10^{-16}
	11704	14162	IA/2014/NADC34	NADC30	8.121×10^{-63}	7.634×10^{-50}	1.473×10^{-57}	7.816×10^{-22}	3.737×10^{-25}	–	1.110×10^{-16}
JS2020	4,921	7,664	JXA1	NADC30	1.008×10^{-51}	–	4.599×10^{-50}	6.777×10^{-22}	8.945×10^{-15}	–	1.110×10^{-16}
	11,670	14,051	IA/2014/NADC34	NADC30	6.430×10^{-57}	2.048×10^{-36}	4.453×10^{-58}	1.264×10^{-05}	3.107×10^{-02}	–	3.330×10^{-16}
PRRSV/CN/FJGD01/20211/2021	4,922	7,668	JXA1	NADC30	5.356×10^{-50}	1.133×10^{-29}	1.341×10^{-46}	4.832×10^{-21}	2.685×10^{-13}	–	1.110×10^{-16}
	11,674	14,055	IA/2014/NADC34	NADC30	1.141×10^{-49}	5.089×10^{-28}	1.130×10^{-50}	3.990×10^{-20}	7.778×10^{-04}	–	3.330×10^{-16}
China/SCcd2020/2020	3,583	4,086	JXA1	NADC30	1.541×10^{-32}	2.144×10^{-24}	1.100×10^{-32}	5.107×10^{-13}	8.306×10^{-14}	–	4.440×10^{-16}
	4,923	7,618	JXA1	NADC30	4.540×10^{-54}	1.644×10^{-40}	3.238×10^{-54}	3.229×10^{-20}	3.582×10^{-23}	–	4.440×10^{-16}
	11,675	14,163	IA/2014/NADC34	NADC30	4.276×10^{-57}	8.068×10^{-38}	7.961×10^{-58}	8.231×10^{-24}	2.620×10^{-17}	–	3.330×10^{-16}
SDIz20-04	4,920	7,677	JXA1	NADC30	1.460×10^{-97}	1.633×10^{-40}	3.899×10^{-96}	2.133×10^{-24}	2.620×10^{-32}	–	4.440×10^{-16}
	11,674	14,217	IA/2014/NADC34	NADC30	6.966×10^{-61}	4.330×10^{-41}	6.873×10^{-61}	2.251×10^{-23}	2.466×10^{-16}	–	4.440×10^{-16}
YC-2020	4,925	7,668	JXA1	NADC30	2.456×10^{-96}	1.335×10^{-36}	3.052×10^{-95}	1.507×10^{-33}	1.049×10^{-21}	–	4.440×10^{-16}
	11,737	14,056	IA/2014/NADC34	NADC30	2.282×10^{-65}	1.509×10^{-49}	3.219×10^{-67}	2.979×10^{-23}	1.019×10^{-24}	–	4.440×10^{-16}

[1)] –, not significant.

identity with JXA1 (Table 3). The homology with the NADC30 strains was relatively high, which was consistent with the results of the genome-wide phylogenetic analysis. The genome-wide homology of L1A variants ranged from 90.0 to 99.5%, and the large homology differences among some strains may have been related to the presence of additional recombinant fragments in some strains. TZJ2756 shares high nucleotide/amino acid homology in the ORF5-ORF7 region with other L1A variants. Therefore, the TZJ2756 strain is an excellent model for evaluating the pathogenicity of L1A variants (Table 3).

3.6. Clinical signs of TZJ2756-infected piglets

All the piglets infected with TZJ2756 exhibited significant clinical symptoms, including persistent fever, cough, anorexia and drowsiness. All piglets in the challenged group had persistent fever (≥40°C) from 3 to 10 dpi (the temperature of some piglets exceeded 40.5°C from 4 to 9 dpi), peaking at 8 dpi at a temperature of 41.3°C, and their body temperature then returned to the normal range at 11 dpi (Fig. 3-A). In contrast, the piglets in the control group exhibited normal behavior and did not show any clinical signs during the entire duration of the experiment. The body weights of the piglets were recorded at 0, 7, 14, and 21 dpi, revealing that the average daily body weight gain in piglets infected with TZJ2756 was significantly lower ($P<0.001$) than that in uninfected piglets during the 8–14-dpi period (Fig. 3-B). All the piglets survived to the end of the experiment.

3.7. PRRSV antibody detection

Serum samples were collected from the piglets to measure the levels of PRRSV N protein antibodies. In the challenge group inoculated with TZJ2756, 2 out of 5 piglets showed seroconversion (S/P>0.4) at 7 dpi, and all the piglets tested positive at 10 dpi. Over time, the levels of PRRSV antibodies gradually increased before 14 dpi and decreased slightly at 21 dpi. In contrast, the control group consistently tested negative (S/P<0.4) throughout the experiment (Fig. 3-C).

3.8. Macroscopic and histopathological lesions

All the piglets were euthanized and autopsied at 21 dpi. In comparison to the piglets in the control group, 2 of 5 piglets in the challenge group exhibited characteristic PRRS lesions, including lung consolidation and lymph node hemorrhaging (Fig. 4-A and B). Histopathological examination of the challenge group revealed interstitial edema and severe interstitial pneumonia in the lungs (Fig. 4-C). Furthermore, increased numbers of lymphatic nodules were observed in the submaxillary lymph nodes of the challenge group (Fig. 4-D). No pathological lesions were observed in the aforementioned tissues of the pigs in the control group.

3.9. Assessment of viremia and viral loads in tissue

The viral load in serum samples from individual piglets was assessed at 3, 5, 7, 10, 14, 17, and 21 dpi.

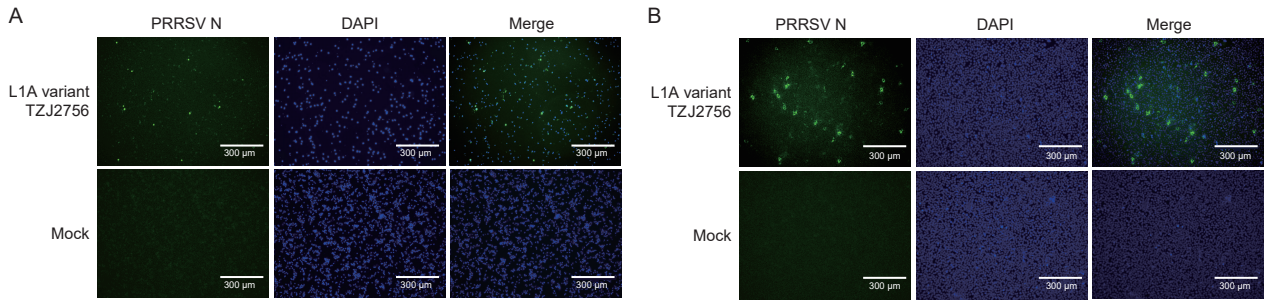


Fig. 2 Immunofluorescence assays (IFAs) images showing the reactivity of a monoclonal antibody against the respiratory syndrome virus (PRRSV) N protein in TZJ2756-infected primary alveolar macrophages (PAMs) (A) and Marc-145 cells (B). The nuclei were stained with DAPI.

Table 3 Nucleotide and amino acid sequence similarity between L1A variants and the reference strains[1)]

Amino acids/ nucleotides	IA/2014/NADC34	NADC30	JXA1	TZJ2756	Among L1A variants
Whole genome	85.0–86.4	88.7–90.7	83.4–85.9	90.9–94.7	90.0–99.5
ORF1a	79.8–81.0/75.5–81.8	85.7–88.9/84.7–89.9	81.0–85.9/75.7–85.5	87.6–99.0/86.5–93.0	87.2–99.4/84.8–99.4
ORF1b	86.7–88.1/94.8–96.0	93.0–94.6/96.9–98.0	85.9–87.3/94.9–95.9	90.9–99.0/96.0–98.6	91.0–99.6/96.0–99.9
ORF2a	87.0–96.0/85.6–94.9	84.2–89.2/80.5–87.5	84.8–86.3/81.7–86.8	87.3–99.1/86.8–98.1	86.0–99.5/83.7–99.6
ORF2b	89.6–97.7/94.6–98.6	86.0–90.5/87.8–90.5	85.6–91.4/83.8–90.5	87.8–99.5/91.9–98.6	86.0–99.5/90.5–98.6
ORF3	93.2–95.3/91.0–94.9	83.9–85.9/82.4–85.1	81.7–83.4/78.0–81.2	93.3–99.5/94.5–98.0	93.1–99.2/91.8–98.8
ORF4	94.2–96.1/93.9–97.8	93.1–95.0/92.7–95.5	84.2–86.6/85.5–89.9	93.9–99.3/93.3–99.4	93.7–99.8/92.7–99.4
ORF5	94.0–97.3/90.5–97.0	86.6–88.2/88.1–91.5	84.9–87.1/85.6–89.1	93.9–98.8/92.0–98.5	93.5–99.2/93.0–98.5
ORF5a	92.9–98.1/92.3–98.1	89.1–92.3/88.5–94.2	83.3–87.8/73.1–80.8	93.6–99.4/92.3–98.1	89.7–99.4/88.5–100.0
ORF6	92.8–97.7/93.1–97.1	93.1–95.2/93.1–97.1	86.9–89.0/90.9–94.9	93.3–98.5/94.9–99.4	93.5–99.0/94.3–100.0
ORF7	92.2–95.2/91.9–94.4	94.4–97.0/94.4–96.0	87.9–90.3/88.7–90.3	96–99.5/96.8–100.0	95.4–100.0/96.0–100.0

[1)] When comparing with TZJ2756 strain, exclude itself.

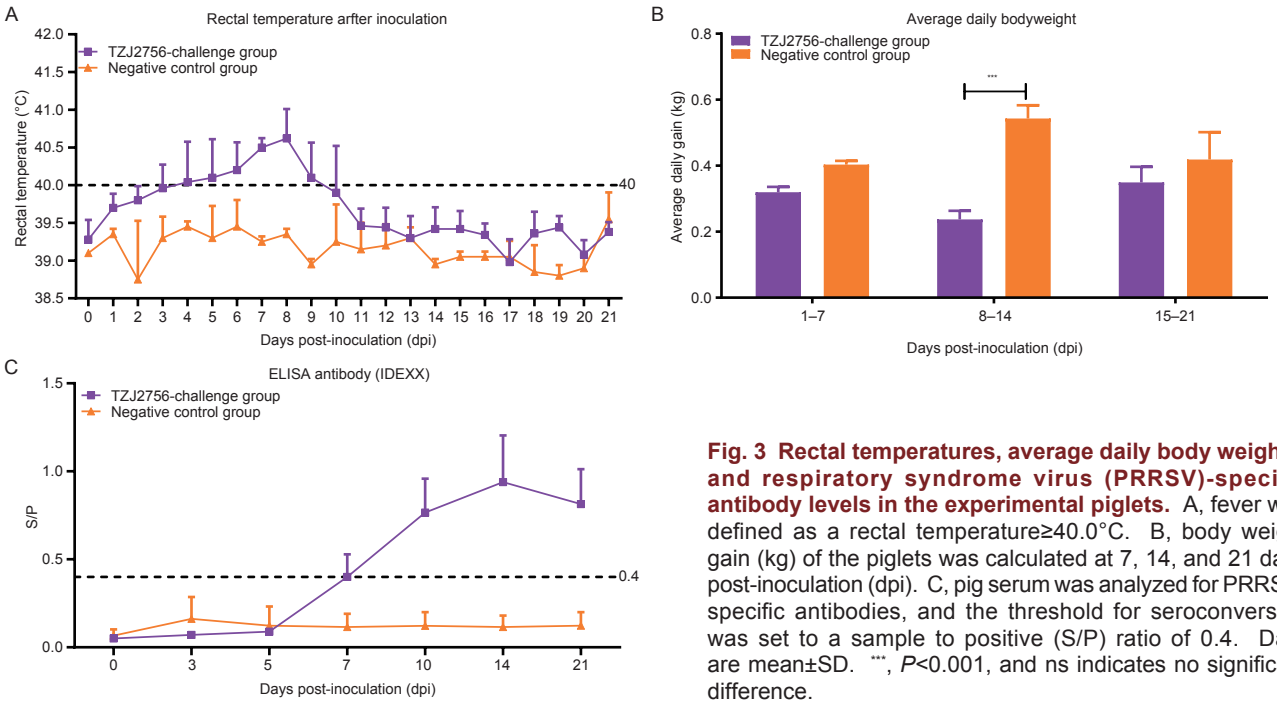


Fig. 3 Rectal temperatures, average daily body weights, and respiratory syndrome virus (PRRSV)-specific antibody levels in the experimental piglets. A, fever was defined as a rectal temperature≥40.0°C. B, body weight gain (kg) of the piglets was calculated at 7, 14, and 21 days post-inoculation (dpi). C, pig serum was analyzed for PRRSV-specific antibodies, and the threshold for seroconversion was set to a sample to positive (S/P) ratio of 0.4. Data are mean±SD. ***, $P<0.001$, and ns indicates no significant difference.

Following infection with TZJ2756, the viral load in the piglets increased rapidly during the 0–3-dpi period, peaking at 3 dpi ($1\times10^{6.13}$ copies mL^{-1}). Subsequently, the viremia started to gradually decrease; although it is noteworthy that all the piglets in the challenge group still exhibited viremia at 21 dpi ($1\times10^{3.82}$ copies mL^{-1}). No viremia was detected in the control group (Fig. 5-A).

The hearts, livers, spleens, lungs, kidneys, stomachs,

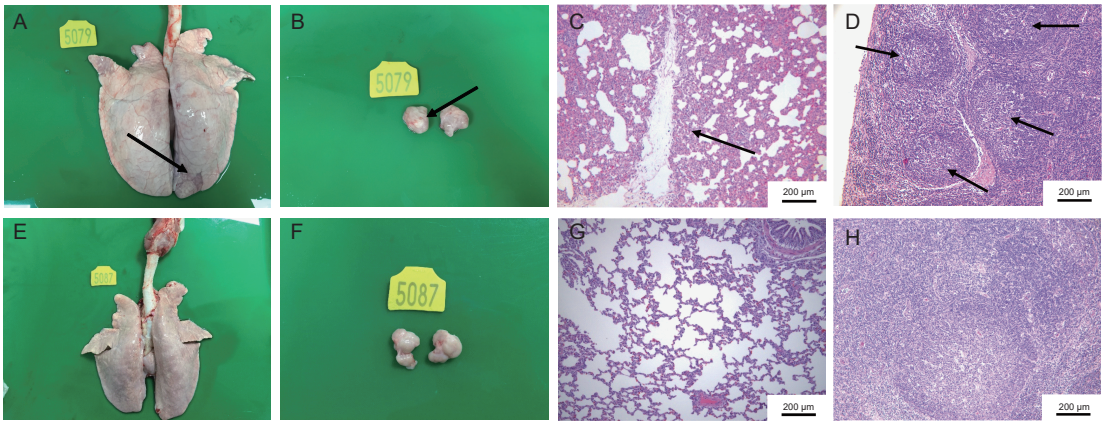


Fig. 4 Pathological examination revealed significant increase in lung lesions (A) and hemorrhage in the submaxillary lymph nodes (B) of the piglets in the challenge group euthanized at 21 days post-inoculation (dpi) compared with those in the control group (E and F). The piglets in the challenge group exhibited interstitial edema and severe interstitial pneumonia in the lungs (C), and the number of lymphatic nodules was increased in the lymph nodes (D); in contrast, those in the control group did not exhibit any significant lesions (G and H). The images were viewed at an original magnification of 200×. The pointer indicates the location of the lesion.

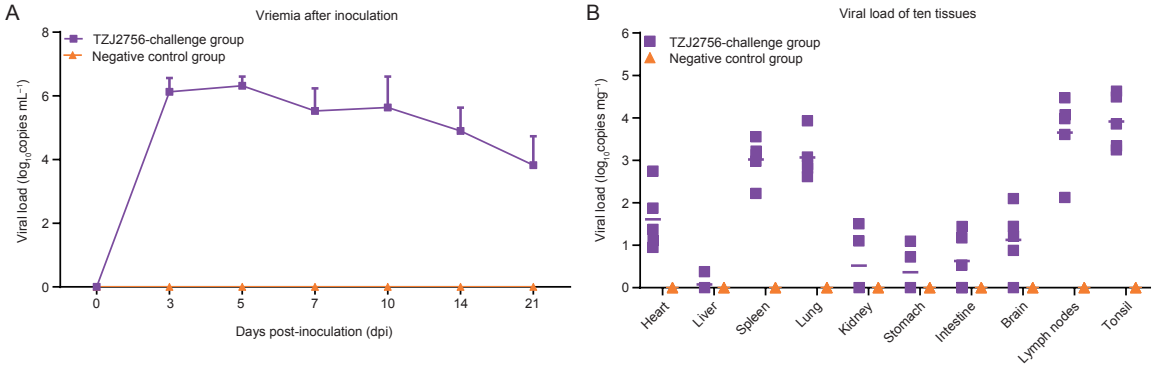


Fig. 5 Viral load and distribution in tissues. The respiratory syndrome virus (PRRSV) viral load in tissues and serum from each group was determined by RT-qPCR. Tissue samples were collected at 21 days post-inoculation (dpi), and serum samples were collected at 0, 3, 7, 10, 14, 17 and 21 dpi. Viremia in the serum (A) and the viral distribution in the tissues (B) of the piglets were detected. Data are mean±SD.

small intestines, brains, submaxillary lymph nodes, and tonsils of individual piglets were subjected to RT-qPCR analysis. The results of the viral load measurements of the tissue samples revealed that the TZJ2756 strain was present in all the collected tissues (Fig. 5-B). Furthermore, the highest viral load was detected in the tonsils and submaxillary lymph nodes of the TZJ2756-infected piglets (Fig. 5-B).

4. Discussion

In 2017, NADC34-like PRRSV was found for the first time in China (Zhang *et al.* 2018). These strains produced many recombinant viruses in a short time and rapidly spread throughout China (Xu *et al.* 2022c; Zhou *et al.* 2022; Yuan *et al.* 2023). By 2021, NADC34-like PRRSV strains, together with HP-PRRSV and NADC30-like strains were the three major epidemic strains in China, which made the epidemic strains of PRRSV in China more complex and diverse (Xu *et al.* 2022a). In this study, we found that a new class of NADC34-like PRRSV strains emerged in China and were named the L1A variant. Moreover, we summarized and analyzed the epidemiological characteristics of the L1A variant, successfully isolated the L1A variant strain TZJ2756, and identified its pathogenicity in piglets.

The high frequency of recombination contributes to the production of new variants that often exhibit strong environmental adaptability (Park *et al.* 2020). Through phylogenetic and recombination analyses, we determined that the L1A variant was a recombinant virus with NADC30-like strains as its main parent and recombinant fragments provided by JXA1-like and NADC34-like PRRSV strains. The ORF2-ORF6 gene fragments were obtained from NADC34-like PRRSV strains. Therefore, based on the ORF5 phylogenetic analysis, the L1A variant was classified as L1A (NADC34-like), but based on the whole-genome sequence analysis, it was classified as L1C (NADC30-like). All L1A variants had three very similar recombination breakpoints located in the Nsp2, Nsp9 and ORF2 gene regions (Table 2; Appendix A). Zhang *et al.* (2019) and Yu *et al.* (2020) reported that the recombination hotspots of PRRSV were located at the nucleotide sites of Nsp9 and GP2-GP3, which was highly consistent with the recombination breakpoint of L1A variants. The recombination of PRRSV in these regions

may be linked to an enhanced replication capacity and cellular tropism, which likely facilitates its survival and spread, ultimately contributing to the pathogenesis of PRRSV (Yu *et al.* 2020).

According to the accumulated data, the pathogenicity of the recombinant PPRSV strains was generally between that of the parental strains (Yu *et al.* 2022). Compared with those of the mildly pathogenic NADC34-like PRRSV HLJDZD32-1901 (Song *et al.* 2020) and LNTZJ1341-2012 (Xu *et al.* 2023) strains isolated by our team without recombination, the pathogenicity of the L1A variant TZJ2756 was significantly greater. TZJ2756 infection caused persistent fever and significantly slowed the weight gain. At autopsy, significant lung consolidation was found, histopathological tests revealed interstitial edema and severe interstitial pneumonia, but no pigs died, and the pathogenicity of TZJ2756 was moderate in piglets. The TZJ2756 strain was distributed throughout all ten organs collected in this study, and the tonsils had the highest load. Several studies have also evaluated the pathogenicity of L1A variants, which also exhibit moderate to high pathogenicity, and concluded that L1A variants can cause long-term high-load viremia and severe histopathological changes in piglets (Liu *et al.* 2022; Wang *et al.* 2022; Wu *et al.* 2022; Zhao *et al.* 2023; Zhou *et al.* 2023) (Table 4). When sows are infected with the L1A variant, the mortality and abortion rates can reach 50% (Wu *et al.* 2022). Because pathogenicity tests are usually conducted in sterile laboratories, infection with L1A variants in the field may have a greater impact on pigs.

To our knowledge, only the L1C variant reported in the United States belongs to a class of viruses with the same recombination pattern that is widely prevalent in a specific region (Fig. 1-D) (Pamornchainavakul *et al.* 2022; Yim-im *et al.* 2023). Several studies have shown that no PRRSV strain in China is highly homologous to L1C variant strains in the United States (Tian *et al.* 2022; Xu *et al.* 2022b). However, we found that many characteristics of the Chinese L1A variant were very similar to those of the American L1C variant: (1) They all formed a separate clade; (2) they all had a characteristic amino-acid-deletion pattern in the Nsp2 region; (3) they spread rapidly in a short period; (4) they all recombined with local dominant strains and had similar or identical recombination patterns; and (5) they all exhibited moderate to high pathogenicity (Table 5). According to the GenBank database, the L1A variant first appeared in 2020, and within only 3 years, the L1A variant had

Table 4 Comparison of the pathogenicity of different L1A variant strains

Infecting PRRSV strain[1)]	Accession number	Days post-inoculation (dpi)	Inoculated dose	Parameters evaluated	Challenge group	References
TZJ2756	OQ748875	21	4×10^5 $TCID_{50}$	Clinical symptoms, days of fever (≥40°C), histopathological lesions viremia	Significant clinical symptoms 7 d, severe histopathological changes, peaked at 3 dpi, longer than 21 d	This study
China/SCcd2020/2020	MW803134	14	$2\times10^{9.19}$ $TCID_{50}$	Clinical symptoms, days of fever (≥40°C), histopathological lesions, viremia	Severe clinical symptoms, 3/5 pigs died, more than 14 d, severe histopathological changes, peaked at 10 dpi, longer than 14 d	Zhou *et al.* (2023)
YC-2020	ON180781	30	4×10^4 $TCID_{50}$	Clinical symptoms days of fever (≥40°C), histopathological lesions, viremia	Mild clinical symptoms, no fever, severe histopathological changes, peaked at 6 dpi, longer than 30 d	Zhao *et al.* (2023)
GXQZ20210403	OK486523	14	2×10^4 $TCID_{50}$	Clinical symptoms, days of fever (≥40°C), pathological and histopathological lesions, viremia	Severe clinical symptoms, 1/5 pigs died, 4 d, severe histopathological changes, peaked at 7 dpi, longer than 14 d	Wang *et al.* (2022)
PRRSV/CN/FJGD01/2021	OL310959	28	4×10^5 $TCID_{50}$	Clinical symptoms, days of fever (≥40°C), pathological and histopathological lesions, viremia	Obvious clinical signs, 14 d, severe histopathological changes, peaked at 11 dpi, longer than 28 d	Liu *et al.* (2022)
GD-H1	ON691479	14	2×10^5 $TCID_{50}$	Clinical symptoms, days of fever (≥40°C), pathological and histopathological lesions, viremia	Obvious clinical signs, 10 d, severe histopathological changes, peaked at 5 dpi, longer than 14 d	Wu *et al.* (2022)
GD-F1	ON691480	14	2×10^5 $TCID_{50}$	Clinical symptoms, days of fever (≥40°C), pathological and histopathological lesions, viremia	Obvious clinical signs, 10 d, severe histopathological changes, peaked at 5 dpi, longer than 14 d	Wu *et al.* (2022)

[1)] PRRSV, porcine reproductive and respiratory syndrome virus.

become prevalent in at least 12 regions, strengthening the epidemiological surveillance of the strain.

5. Conclusion

In brief, a new clade of NADC34-like and NADC30-like PRRSV strains emerged in China and was named the L1A variant. The L1A variant strains are a class of recombinant viruses that contain a viral skeleton obtained from NADC30-like strains and a partial recombination fragment obtained from the NADC34-like and JXA1-like strains, which exhibit similar viral recombination patterns and have the same characteristic 131-aa deletion in the Nsp2 region. The L1A variant TZJ2756 exhibits moderate pathogenicity and could cause prolonged high-load viremia in infected piglets. Our findings contribute to the understanding of the evolutionary characteristics of Chinese NADC34-like PRRSV strains and provide data on L1A variants in China.

Acknowledgements

This study was supported by grants from the National Natural Science Foundation of China (32172890 and 32002315), the National Key Research and Development Program of China (2022YFF0711004), the Natural Science Foundation of Heilongjiang Province, China (YQ2022C042), the State Key Laboratory of Veterinary Biotechnology Foundation of China (SKLVBF202208), the Postdoctoral Fellowship Program of CPSF, China (GZC20233062) and the National Center of Technology Innovation for Pigs, China (NCTIP-XD/C09).

Declaration of competing interest

The authors declare that they have no conflict of interest.

Declaration of generative AI and AI-assisted technologies in the writing process

The authors declare that they did not use AI in the preparation and writing of this manuscript.

Ethical approval

This study was approved by the Animal Ethics Committee of the School of Harbin Veterinary Research Institute of the Chinese Academy of Agricultural Sciences and was performed in accordance with animal ethics guidelines and approved protocols. The Animal Ethics Committee approval number was SYXK (Hei) 2011022.

Table 5 Comparison of the characteristics of American L1C and Chinese L1A variants

Epidemic characteristics	American L1C variant	Chinese L1A variant
Formed a separate clade	Yes	Yes
aa-deletion of Nsp2 protein	Yes (100-aa deletion)	Yes (131-aa deletion (19+1+111))
Became widespread in a short period	Yes	Yes
Underwent recombination with local strains	Yes	Yes
Recombination patterns	Consistent recombination characteristics	Similar recombination characteristics
ORF5 gene similarity among strains	High (≥98%)	Higher (≥93%)
Pathogenicity	High pathogenicity	Moderate to high pathogenicity

Appendix associated with this study is available at https://doi.org/10.1016/j.jia.2024.03.056

References

de Abin M F, Spronk G, Wagner M, Fitzsimmons M, Abrahante J E, Murtaugh M P. 2009. Comparative infection efficiency of Porcine reproductive and respiratory syndrome virus field isolates on MA104 cells and porcine alveolar macrophages. *Canadian Journal of Veterinary Research-Revue Canadienne De Recherche Veterinaire*, **73**, 200–204.

Brinton M A, Gulyaeva A A, Balasuriya U B R, Dunowska M, Faaberg K S, Goldberg T, Leung F C C, Nauwynck H J, Snijder E J, Stadejek T, Gorbalenya A E. 2021. ICTV virus taxonomy profile: Arteriviridae 2021. *Journal of General Virology*, **102**, 001632.

Cui X Y, Xia D S, Huang X Y, Sun Y, Shi M, Zhang J Q, Li G W, Yang Y B, Wang H W, Cai X H, An T Q. 2022. Analysis of recombinant characteristics based on 949 PRRSV-2 genomic sequences obtained from 1991 to 2021 shows that viral multiplication ability contributes to dominant recombination. *Microbiology Spectrum*, **10**, e0293422.

Guo Z H, Chen X X, Li R, Qiao S L, Zhang G P. 2018. The prevalent status and genetic diversity of porcine reproductive and respiratory syndrome virus in China: A molecular epidemiological perspective. *Virology Journal*, **15**, 2.

Guo Z H, Chen X X, Li X, Qiao S L, Deng R G, Zhang G P. 2019. Prevalence and genetic characteristics of porcine reproductive and respiratory syndrome virus in central China during 2016–2017: NADC30-like PRRSVs are predominant. *Microbial Pathogenesis*, **135**, 103657.

Katoh K, Standley D M. 2013. MAFFT multiple sequence alignment software version 7: Improvements in performance and usability. *Molecular Biology and Evolution*, **30**, 772–780.

Kikuti M, Paploski I A D, Pamornchainavakul N, Picasso Risso C, Schwartz M, Yeske P, Leuwerke B, Bruner L, Murray D, Roggow B D, Thomas P, Feldmann L, Allerson M, Hensch M, Bauman T, Sexton B, Rovira A, VanderWaal K, Corzo C A. 2021. Emergence of a new lineage 1C variant of porcine reproductive and respiratory syndrome virus 2 in the United States. *Frontiers in Veterinary Science*, **8**, 752938.

Kim S C, Kim H J, Moon S H, Cho H S, Kim W I. 2023. First identification and genomic characterization of NADC34-Like PRRSV strains isolated from MLV-vaccinated pigs in Korea. *Transboundary and Emerging Diseases*, **2023**, 9995433.

Kumar S, Stecher G, Tamura K. 2016. MEGA7: Molecular evolutionary genetics analysis version 7.0 for bigger datasets. *Molecular Biology and Evolution*, **33**, 1870–1874.

Lee M A, Jayaramaiah U, You S H, Shin E G, Song S M, Ju L J, Kang S J, Hyun B H, Lee H S. 2023. Molecular characterization of porcine reproductive and respiratory syndrome virus in korea from 2018 to 2022. *Pathogens*, **12**, 757.

Leng C L, An T Q, Chen J Z, Gong D Q, Peng J M, Yang Y Q, Wu J, Guo J J, Li D Y, Zhang Y, Meng Z X, Wu Y Q, Tian Z J, Tong G Z. 2012. Highly pathogenic porcine reproductive and respiratory syndrome virus GP5 B antigenic region is not a neutralizing antigenic region. *Veterinary Microbiology*, **159**, 273–281.

Li W S, Li M H, Zhang H L, Li C, Xu H, Gong B J, Fu J, Guo Z Y, Peng J M, Zhou G H, Tian Z J, Wang Q. 2022. A novel immunochromatographic strip based on latex microspheres for the rapid detection of north american-type porcine reproductive and respiratory syndrome virus. *Frontiers in Microbiology*, **13**, 882112.

Li Y H, Tas A, Sun Z, Snijder E J, Fang Y. 2015. Proteolytic processing of the porcine reproductive and respiratory syndrome virus replicase. *Virus Research*, **202**, 48–59.

Liu J K, Liu C, Xu Y, Yang Y, Li J R, Dai A L, Huang C Q, Luo M L, Wei C H. 2022. Molecular characteristics and pathogenicity of a novel recombinant porcine reproductive and respiratory syndrome virus strain from nadc30-, nadc34-, and jxa1-like strains that emerged in China. *Microbiology Spectrum*, **10**, e0266722.

Murtaugh M P, Stadejek T, Abrahante J E, Lam T T Y, Leung F C C. 2010. The ever-expanding diversity of porcine reproductive and respiratory syndrome virus. *Virus Research*, **154**, 18–30.

Nathues H, Alarcon P, Rushton J, Jolie R, Fiebig K, Jimenez M, Geurts V, Nathues C. 2017. Cost of porcine reproductive and respiratory syndrome virus at individual farm level—An economic disease model. *Preventive Veterinary Medicine*, **142**, 16–29.

Pamornchainavakul N, Kikuti M, Paploski I A D, Makau D N, Rovira A, Corzo C A, VanderWaal K. 2022. Measuring how recombination re-shapes the evolutionary history of PRRSV-2: A genome-based phylodynamic analysis of the emergence of a novel prrsv-2 variant. *Frontiers in Veterinary Science*, **9**, 846904.

Paploski I A D, Pamornchainavakul N, Makau D N, Rovira A, Corzo C A, Schroeder D C, Cheeran M C J, Doeschl-Wilson A, Kao R D R, Lycett S, VanderWaal K. 2021. Phylogenetic structure and sequential dominance of sub-lineages of prrsv type-2 lineage 1 in the united states. *Vaccines*, **9**, 608.

Park J, Choi S, Jeon J H, Lee K W, Lee C. 2020. Novel lineage 1 recombinants of porcine reproductive and respiratory syndrome virus isolated from vaccinated herds: Genome sequences and cytokine production profiles. *Archives of Virology*, **165**, 2259–2277.

Shi M, Holmes E C, Brar M S, Leung F C C. 2013. Recombination is associated with an outbreak of novel highly pathogenic porcine reproductive and respiratory syndrome viruses in China. *Journal of Virology*, **87**, 10904–10907.

Shi M, Lam T T Y, Hon C C, Hui R K H, Faaberg K S, Wennblom T, Murtaugh M P, Stadejek T, Leung F C C. 2010a. Molecular epidemiology of PRRSV: A phylogenetic perspective. *Virus Research*, **154**, 7–17.

Shi M, Lam T T Y, Hon C C, Murtaugh M P, Davies P R, Hui R K H, Li J, Wong L T W, Yip C W, Jiang J W, Leung F C C. 2010b. Phylogeny-based evolutionary, demographical, and geographical dissection of north american type 2 porcine reproductive and respiratory syndrome viruses. *Journal of Virology*, **84**, 8700–8711.

Song S J, Xu H, Zhao J, Leng C L, Xiang L R, Li C, Fu J, Tang Y D, Peng J M, Wang Q, Zhao H Y, An T Q, Cai X H, Zhang H L, Tian Z J. 2020. Pathogenicity of NADC34-like PRRSV HLJDZD32-1901 isolated in China. *Veterinary Microbiology*, **246**, 108727.

Sun Q, Xu H, An T Q, Cai X H, Tian Z J, Zhang H L. 2023. Recent progress in studies of porcine reproductive and respiratory syndrome virus 1 in china. *Viruses-Basel*, **15**, 1528.

Tian X, Huang X, Xia D, Wang H, Tian Z, Cai X, An T. 2022. Isolation, identification and epidemiological analysis of RFLP 1-4-4 L1C strain of porcine reproductive and respiratory syndrome virus. *Chinese Journal of Preventive Veterinary Medicine*, **44**, 583–590. (in Chinese)

Trevisan G, Li G W, Moura C A A, Coleman K, Thomas P, Zhang J Q, Gauger P, Zeller M, Linhares D. 2021a. Complete coding genome sequence of a novel porcine reproductive and respiratory syndrome virus 2 restriction fragment length polymorphism 1-4-4 lineage 1c variant identified in Iowa, USA. *Microbiology Resource Announcements*, **10**, e0044821.

Trevisan G, Sharma A, Gauger P, Harmon K M, Zhang J Q, Main R, Zeller M, Linhares L C M, Linhares D C L. 2021b. PRRSV2 genetic diversity defined by RFLP patterns in the United States from 2007 to 2019. *Journal of Veterinary Diagnostic Investigation*, **33**, 920–931.

Wang X D, Zhang K, Mo Q R, Chen G C, Lv J, Huang J, Pang Y L, Wang H, Liu W B, Huang K, Min X L, Ren T W, Ouyang K, Chen Y, Huang W J, Wei Z Z. 2022. The emergence and pathogenesis of recombinant viruses associated with nadc34-like strains and the predominant circulating strains of porcine reproductive and respiratory syndrome virus in southern china. *Viruses-Basel*, **14**, 1695.

Wu Y, Peng O, Xu Q P, Li Q H, Li W, Lin L M, Zhou Q F, Cai X B, Hu G L, He Z Y, Chen Y S, Zhang H. 2022. Characterization and pathogenicity of two novel PRRSVs recombined by NADC30-like and NADC34-like strains in China. *Viruses-Basel*, **14**, 2174.

Xu H, Gong B, Li C, Sun Q, Li W, Zhao J, Guo Z, Li J, Zhang S, Xiang L, Peng J, Wang Q, Zhou G, Leng C, Tang Y, Zhao H, An T, Cai X, Zhang H, Tian Z. 2022c. Analysis of the emergence and epidemic status of new L1A PRRSV variants in China. *Chinese Journal of Preventive Veterinary Medicine*, **45**, 779–786. (in Chinese)

Xu H, Li C, Gong B J, Li W S, Guo Z Y, Sun Q, Zhao J, Xiang L R, Li J H, Tang Y D, Leng C L, Wang Q, Peng J M, Zhou G H, Liu H R, An T Q, Cai X H, Tian Z J, Zhang H L. 2023. Protective efficacy of a candidate live-attenuated vaccine derived from the SD-R strain against NADC34-like porcine reproductive and respiratory syndrome virus. *Vaccines*, **11**, 1349.

Xu H, Li C, Li W S, Zhao J, Gong B J, Sun Q, Tang Y D, Xiang L R, Leng C L, Peng J M, Wang Q, Meng F D, Yu Y, An T Q, Cai X H, Tian Z J, Zhang H L. 2022a. Novel characteristics of Chinese NADC34-like PRRSV during 2020–2021. *Transboundary and Emerging Diseases*, **69**, E3215-E3224.

Xu H, Li C, Xiang L, Tang Y, Zhao J, Gong B, Li W, Fu J, Peng J, Wang Q, Zhou G, Leng C, An T, Cai X, Zhang H, Tian Z. 2022b. Whole genome sequence analysis of the same subtype branch of lineage1C PRRSV variant (ORF5 RFLP 1-4-4) between China and United States. *Chinese Journal of Preventive Veterinary Medicine*, **44**, 202–207. (in Chinese)

Xu H, Song S, Zhao J, Leng C, Fu J, Li C, Tang Y D, Xiang L, Peng J, Wang Q, Zhao H, An T, Cai X, Zhang H, Tian Z J. 2020. A potential endemic strain in China: NADC34-like porcine reproductive and respiratory syndrome virus. *Transboundary and Emerging Diseases*, **67**, 1730–1738.

Yim-im W, Anderson T K, Paploski I A D, Vanderwaal K, Gauger P, Krueger K, Shi M, Main R, Zhang J Q, Chao D Y. 2023. Refining PRRSV-2 genetic classification based on global ORF5 sequences and investigation of their geographic distributions and temporal changes. *Microbiology Spectrum*, **11**, e0291623.

Yu F, Yan Y, Shi M, Liu H Z, Zhang H L, Yang Y B, Huang X Y, Gauger P C, Zhang J Q, Zhang Y H, Tong G Z, Tian Z J, Chen J J, Cai X H, Liu D, Li G W, An T Q. 2020. Phylogenetics, genomic recombination, and NSP2 polymorphic patterns of porcine reproductive and respiratory syndrome virus in China and the United States in 2014–2018. *Journal of Virology*, **94**, e0181319.

Yu Y, Zhang Q Y, Cao Z, Tang Y D, Xia D S, Wang G, Shan H. 2022. Recent advances in porcine reproductive and respiratory syndrome virus NADC30-Like research in China: Molecular characterization, pathogenicity, and control. *Frontiers in Microbiology*, **12**, 791313.

Yuan L L, Zhu Z B, Fan J, Li Q, Liu P R, Li X D. 2023. Efficacy of a commercial prrsv vaccine on NADC34-Like PRRSV challenge. *Transboundary and Emerging Diseases*, **2023**, 4509261.

Zhang H L, Leng C L, Ding Y S, Zhai H Y, Li Z, Xiang L R, Zhang W L, Liu C X, Li M H, Chen J Z, Bai Y, Kan Y C, Yao L G, Peng J M, Wang Q, Tang Y D, An T Q, Cai X H, Tian Z J, Tong G Z. 2019. Characterization of newly emerged NADC30-like strains of porcine reproductive and respiratory syndrome virus in China. *Archives of Virology*, **164**, 401–411.

Zhang H L, Xiang L R, Xu H, Li C, Tang Y D, Gong B J, Zhang W L, Zhao J, Song S J, Peng J M, Wang Q, An T Q, Cai X H, Tian Z J. 2022. Lineage 1 porcine reproductive and respiratory syndrome virus attenuated live vaccine provides broad cross-protection against homologous and heterologous NADC30-Like virus challenge in piglets. *Vaccines*, **10**, 752.

Zhang H L, Zhang W L, Xiang L R, Leng C L, Tian Z J, Tang Y D, Cai X H. 2018. Emergence of novel porcine reproductive and respiratory syndrome viruses (ORF5 RFLP 1-7-4 viruses) in China. *Veterinary Microbiology*, **222**, 105–108.

Zhao H Z, Wang F X, Han X Y, Guo H, Liu C Y, Hou L N, Wang Y X, Zheng H, Wang L, Wen Y J. 2022. Recent advances in the study of NADC34-like porcine reproductive and respiratory syndrome virus in China. *Frontiers in Microbiology*, **13**, 950402.

Zhao Y X, Wang R Q, Li W, Yu C F, Zhang R T, Hu R C, Guo R H, Yang Z Q, Zhou Y F, Wang X L. 2023. Genetic and pathogenic characterization of an NADC-34-like isolate of porcine reproductive and respiratory syndrome virus. *Archives of Virology*, **168**, 205.

Zhou L, Wang Z C, Ding Y P, Ge X N, Guo X, Yang H C. 2015. NADC30-like strain of porcine reproductive and respiratory syndrome virus, China. *Emerging Infectious Diseases*, **21**, 2256–2257.

Zhou L, Yu J F, Zhou J, Long Y P, Xiao L, Fan Y D, Yang D J, Zhang B, Zhang Z D, Liu J. 2023. A novel NADC34-like porcine reproductive and respiratory syndrome virus 2 with complex genome recombination is highly pathogenic to piglets. *Infection Genetics and Evolution*, **112**, 105436.

Zhou L J, Yang Y, Xia Q Q, Guan Z X, Zhang J J, Li B B, Qiu Y F, Liu K, Shao D H, Ma Z Y, Wang X D, Wei J C. 2022. Genetic characterization of porcine reproductive and respiratory syndrome virus from Eastern China during 2017–2022. *Frontiers in Microbiology*, **13**, 971817.

Executive Editor-in-Chief Dongming Zhao
Managing Editor Han Zhang